

**SANDIA REPORT**

SAND2021-9722

Printed Click to enter a date



Sandia  
National  
Laboratories

# Validation of the SCEPTRÉ Boltzmann-CSD Solver

Clifton R. Drumm and Wesley C. Fan

Prepared by  
Sandia National Laboratories  
Albuquerque, New Mexico  
87185 and Livermore,  
California 94550

Issued by Sandia National Laboratories, operated for the United States Department of Energy by National Technology & Engineering Solutions of Sandia, LLC.

**NOTICE:** This report was prepared as an account of work sponsored by an agency of the United States Government. Neither the United States Government, nor any agency thereof, nor any of their employees, nor any of their contractors, subcontractors, or their employees, make any warranty, express or implied, or assume any legal liability or responsibility for the accuracy, completeness, or usefulness of any information, apparatus, product, or process disclosed, or represent that its use would not infringe privately owned rights. Reference herein to any specific commercial product, process, or service by trade name, trademark, manufacturer, or otherwise, does not necessarily constitute or imply its endorsement, recommendation, or favoring by the United States Government, any agency thereof, or any of their contractors or subcontractors. The views and opinions expressed herein do not necessarily state or reflect those of the United States Government, any agency thereof, or any of their contractors.

Printed in the United States of America. This report has been reproduced directly from the best available copy.

Available to DOE and DOE contractors from

U.S. Department of Energy  
Office of Scientific and Technical Information  
P.O. Box 62  
Oak Ridge, TN 37831

Telephone: (865) 576-8401  
Facsimile: (865) 576-5728  
E-Mail: [reports@osti.gov](mailto:reports@osti.gov)  
Online ordering: <http://www.osti.gov/scitech>

Available to the public from

U.S. Department of Commerce  
National Technical Information Service  
5301 Shawnee Rd  
Alexandria, VA 22312

Telephone: (800) 553-6847  
Facsimile: (703) 605-6900  
E-Mail: [orders@ntis.gov](mailto:orders@ntis.gov)  
Online order: <https://classic.ntis.gov/help/order-methods/>



## ABSTRACT

A new Boltzmann-CSD solver has been developed within the SCEPTR<sup>E</sup> radiation-transport code, based on the 1<sup>st</sup>-order form of the transport equation, using discontinuous finite elements in space and energy and discrete ordinates in angle. The Boltzmann-CSD solver has been validated against experimental data for electron energy deposition distributions and for electron emission spectra. Comparison of the calculated results with experimental data shows excellent agreement for many of the test configurations and reasonable agreement for other test configurations. The tests have also been modeled with the ITS Monte Carlo code, which also shows excellent to reasonable agreement with the SCEPTR<sup>E</sup> results and experimental data. The SCEPTR<sup>E</sup> Boltzmann-CSD solver relies on electron cross sections generated by the legacy CEPXS code, which currently is limited to electron-only Boltzmann-CSD cross sections. Performing full electron-photon radiation transport with the Boltzmann-CSD solver will require further development in the cross section generating code. For the energy-deposition calculations, neglecting photon transport results in at most about 5% overprediction of the energy deposition for high-energy electrons on high-Z targets, and relatively insignificant difference for the other test configurations.

## **ACKNOWLEDGEMENTS**

The authors express appreciation to Ron Kensek for helpful discussions regarding the uncertainties in the measurements and the Monte Carlo calculations.

## CONTENTS

1. Background .....	8
2. Results .....	9
2.1. Rester data: total electron emission.....	9
2.2. Rester data: electron emission spectra.....	10
2.3. Rester data: sensitivity to target thickness and source energy.....	19
2.4. Lockwood data: energy deposition profiles .....	21
3. Summary and conclusions .....	28

## LIST OF FIGURES

Figure 2-1 1-MeV electrons on 0.2-range Al.....	11
Figure 2-2 1-MeV electrons on 0.4-range Al.....	12
Figure 2-3 1-MeV electrons on 0.6-range Al.....	13
Figure 2-4 2.5-MeV electrons on 0.2-range Al.....	14
Figure 2-5 2.5-MeV electrons on 0.4-range Al.....	15
Figure 2-6 1-MeV electrons on 0.2-range Au.....	16
Figure 2-7 1-MeV electrons on 0.4-range Au.....	17
Figure 2-8 2.5-MeV electrons on 0.2-range Au.....	18
Figure 2-9 2.5-MeV electrons on 0.4-range Au.....	19
Figure 2-10 2.5-MeV electrons on 0.2-range Au with scaled target thickness .....	20
Figure 2-11 1-MeV electrons on 0.4-range Au with scaled target thickness .....	21
Figure 2-12 Nominal 2.5 MeV electrons on 0.2-range Au.....	22
Figure 2-13 1.033-MeV electrons on range-thick beryllium .....	23
Figure 2-14 1.033-MeV electrons on range-thick aluminum .....	24
Figure 2-15 0.109-MeV electrons on range-thick beryllium .....	25
Figure 2-16 0.314-MeV electrons on range-thick aluminum .....	26
Figure 2-17 0.3-MeV electrons on range-thick copper .....	27
Figure 2-18 0.314-MeV electrons on range-thick tantalum .....	28

## LIST OF TABLES

Table 2-1. Total electron emission with nominal target thickness and electron energy .....	9
--	---

This page left blank

## ACRONYMS AND DEFINITIONS

Abbreviation	Definition
CSD	continuous slowing down
MG	multi-group
$S_N$	discrete ordinates
SAAF	self-adjoint angular flux
LD	linear discontinuous
LC	linear continuous
QOI	quantity of interest
C/E	calculation to experiment ratio

## 1. BACKGROUND

A new solver option has been developed within the SCEPTR<sup>E</sup> radiation transport code [1] that is appropriate for charged-particle transport, e.g. electron, positron or proton transport. The new method can serve as a replacement for the legacy method developed by Morel, et al. [2] that was implemented in the CEPXS cross section generating code [3]. The legacy method allowed neutral-particle radiation transport codes to model charged-particle transport, by using the specialized CEPXS cross sections. The new solver has been validated for two quantities of interest (QOI), the energy deposition distribution for electrons incident on various materials and the electron emission spectra for electrons incident on various materials. The cross sections generated by CEPXS are currently limited to electron-only Boltzmann-CSD cross sections. Performing full electron-photon radiation transport with the Boltzmann-CSD solver will require further development in the cross section generating code.

Neutral-particle radiation is accurately modeled with the Boltzmann transport equation [4]

$$\Omega \cdot \nabla \psi + \sigma_t \psi = \int_{E_{cut}}^{E_{max}} \int_{4\pi} \sigma_s(\Omega' \rightarrow \Omega, E' \rightarrow E) \psi(\mathbf{r}, \Omega', E') d\Omega' dE' + Q, \quad 1-1$$

where  $\mathbf{r}$  is the spatial position,  $\Omega$  is the particle direction of motion, and  $E$  is the particle energy,  $\psi(\mathbf{r}, \Omega, E)$  is the angular flux as a function of space-angle-energy phase space.  $\sigma_t$  is the total cross section,  $\sigma_s(\Omega' \rightarrow \Omega, E' \rightarrow E)$  is the differential scattering cross section in angle and energy, and  $Q$  is a fixed source term.  $E_{cut}$  is the lower-energy cutoff and  $E_{max}$  is the upper energy boundary.

For charged-particle transport, the differential scattering cross section is extremely forward peaked, so it is a common approximation to separate out a continuous-slowing-down (CSD) term that results in energy loss without direction change [5]. The Boltzmann-CSD equation is

$$\Omega \cdot \nabla \psi + \sigma_t \psi - \frac{\partial S \psi}{\partial E} = \int_E^{E_{max}} \int_{4\pi} \sigma_s(\Omega' \rightarrow \Omega, E' \rightarrow E) \psi(\mathbf{r}, \Omega', E') d\Omega' dE' + Q, \quad 1-2$$

where  $S$  is the stopping power, and the extreme forward-peaked part of the scattering cross section has been approximated by the CSD term.

In this work, the Boltzmann-CSD equation is solved using the 1<sup>st</sup>-order form of the transport equation using discontinuous spatial and energy finite elements and discrete-ordinates ( $S_N$ ) in angle. The method can use either linear or quadratic finite elements in space and energy. J. Powell, et al. previously developed a Boltzmann-CSD solver based on the Self-Adjoint Angular Flux (SAAF) form of the transport equation, with linear-discontinuous (LD) energy differencing and linear-continuous (LC) spatial finite elements [6]. The SAAF form of the transport equation breaks down in void regions, so use of the 1<sup>st</sup>-order form of the transport equation is more generally usable. Also, the use of discontinuous spatial finite elements and the availability of higher-order finite elements is generally more accurate for transport applications.

## 2. RESULTS

The Boltzmann-CSD solver in SCEPTR<sup>E</sup> has been compared with experiment for transmitted electron emission spectra and energy deposition for electron-beam sources, and also with ITS Monte Carlo results [7]. Rester, et al. [8] measured the electron emission spectra and total electron emission for source electrons with energies of 1 MeV and 2.5 MeV incident upon  $\sim$ 0.2-0.6 range fraction of Al, Sn and Au. The Rester measurements were initially done in support of radiation shielding design for spacecraft, and the results have been widely used to validate electron transport capabilities.

Lockwood, et al. [9] measured the energy deposition profiles and total energy depositions for electrons of energies from 0.1 MeV to 1.0 MeV on various single materials including atomic numbers from Be to U and multi-material layers. The Lockwood data has also been extensively used to validate electron transport capabilities.

### 2.1. Rester data: total electron emission

Two target materials are considered for these comparisons, Al and Au, and two electron-beam source energies are considered, 1 MeV and 2.5 MeV. Several target thicknesses are considered, of approximately 0.2-, 0.4- and 0.6 fraction of an electron range for the source energy under consideration. The calculated total electron current transmitted and the electron current spectra are compared with measurements in the following tables and plots. For each thickness, the Rester document provides both an approximate range fraction and the corresponding areal density ( $\text{g}/\text{cm}^2$ ) of the target, which are not exactly consistent. For the calculational results presented here, the reported areal densities are used for the target thicknesses, assumed to be the more accurate value. The SCEPTR<sup>E</sup> runs used 50 linear spatial elements,  $S_{16}$  angular quadrature with  $P_7$  scattering, and 200 linear energy groups, which results in numerical errors much less than the reported experimental uncertainty. The ITS calculations were run with sufficient histories such that the statistical uncertainties were much less than the reported experimental uncertainties.

The experimental results report about a 10% error, which are the error bounds included in the tables and plots. The results for nominal target thickness and source electron energies are listed in Table 2-1, showing good agreement except for the 1-MeV electrons on gold targets, where the SCEPTR<sup>E</sup> and ITS calculations are significantly lower than the measured values. The SCEPTR<sup>E</sup> and ITS results are in excellent agreement for all experimental configurations.

**Table 2-1. Total electron emission with nominal target thickness and electron energy**

Target material	Source energy (MeV)	Range fraction	Total emission			SCEPTR <sup>E</sup> C/E
			Rester	ITS	SCEPTR <sup>E</sup>	
Al	1.0	0.2	0.98 $\pm$ 0.1	0.97	0.96	0.98
	“	0.4	0.69 $\pm$ 0.07	0.63	0.63	0.91
	“	0.6	0.27 $\pm$ 0.03	0.27	0.28	1.0
“	2.5	0.2	0.90 $\pm$ 0.09	1.0	1.0	1.1
	“	0.4	0.68 $\pm$ 0.07	0.75	0.76	1.1
	Au	1.0	0.2	0.43 $\pm$ 0.04	0.35	0.35
“	“	0.4	0.04 $\pm$ 0.004	0.025	0.025	0.63
	“	2.5	0.2	0.48 $\pm$ 0.05	0.52	0.53

Target	Source	Range	Total emission			SCEPTRE
“	“	0.4	0.09±0.009	0.094	0.096	1.1

## 2.2. Rester data: electron emission spectra

The electron emission spectra for 1.0 and 2.5 MeV source electron energies on various thicknesses of Al and Au are shown below, with the Rester measured values compared with SCEPTRE and ITS calculated values. The plots include 10% error bounds on the measured data, which is the approximate error reported in the test report. The Rester document states that the experimental uncertainties may increase to ~30% for portions of the spectra that are ~10% of the peak values, but for simplicity, the error bars indicated on the plots are 10% for all data. The agreement between experiment and SCEPTRE and ITS calculations is generally good, with a few exceptions. In the following section, some rudimentary sensitivity analysis is performed, by slightly modifying source electron energy and target thickness, in an attempt to bring the calculations into better agreement with the measurements and as an indication of the sensitivity of the results to the source energy and target thickness. Modification of the source energy and/or target thickness by a few percent significantly affects the calculated electron emission spectra. Uncertainties in source energies and target thicknesses are not included in the test report, but it is plausible that these uncertainties may account for much of the difference between calculation and measurement.

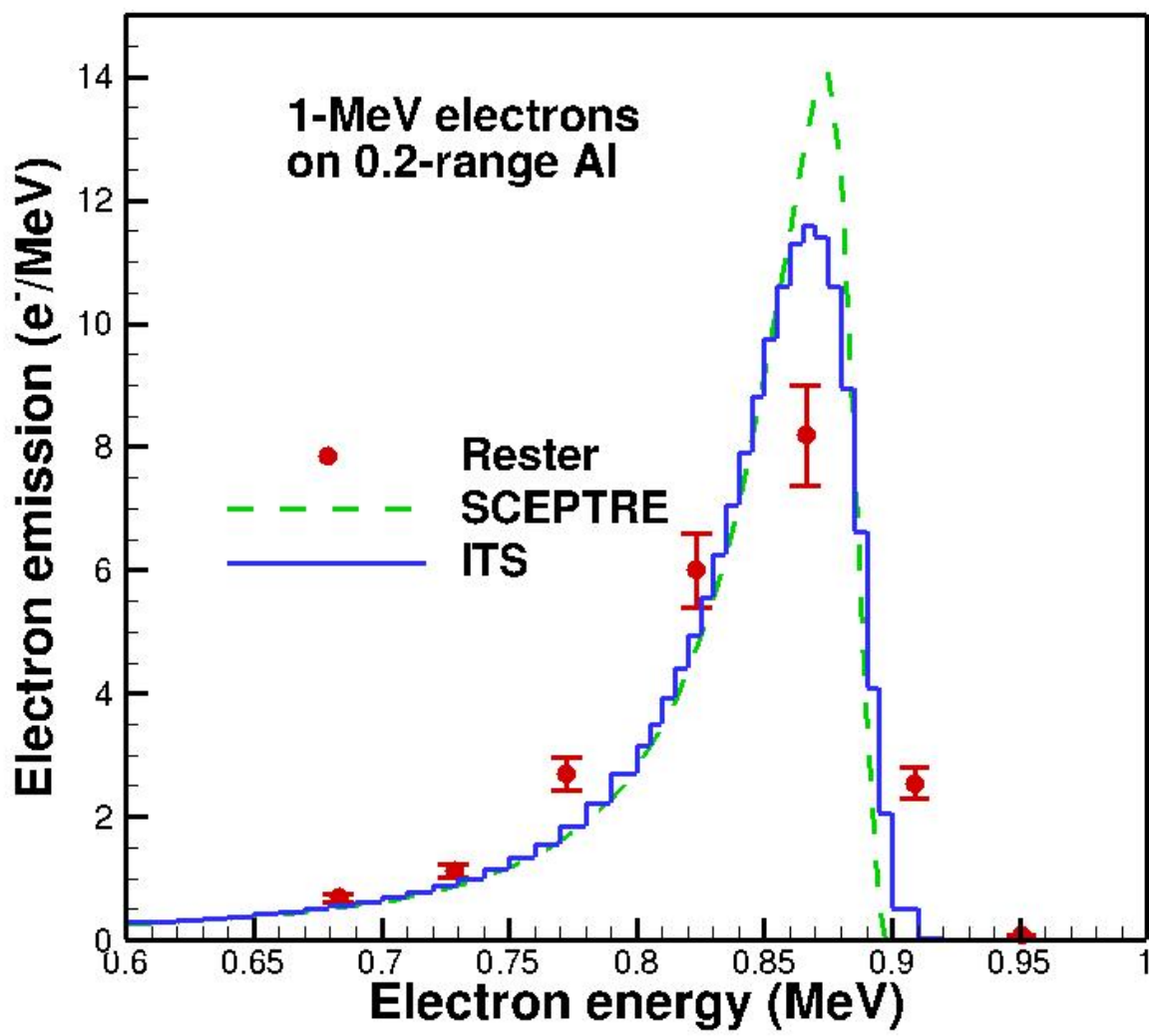


Figure 2-1 1-MeV electrons on 0.2-range Al

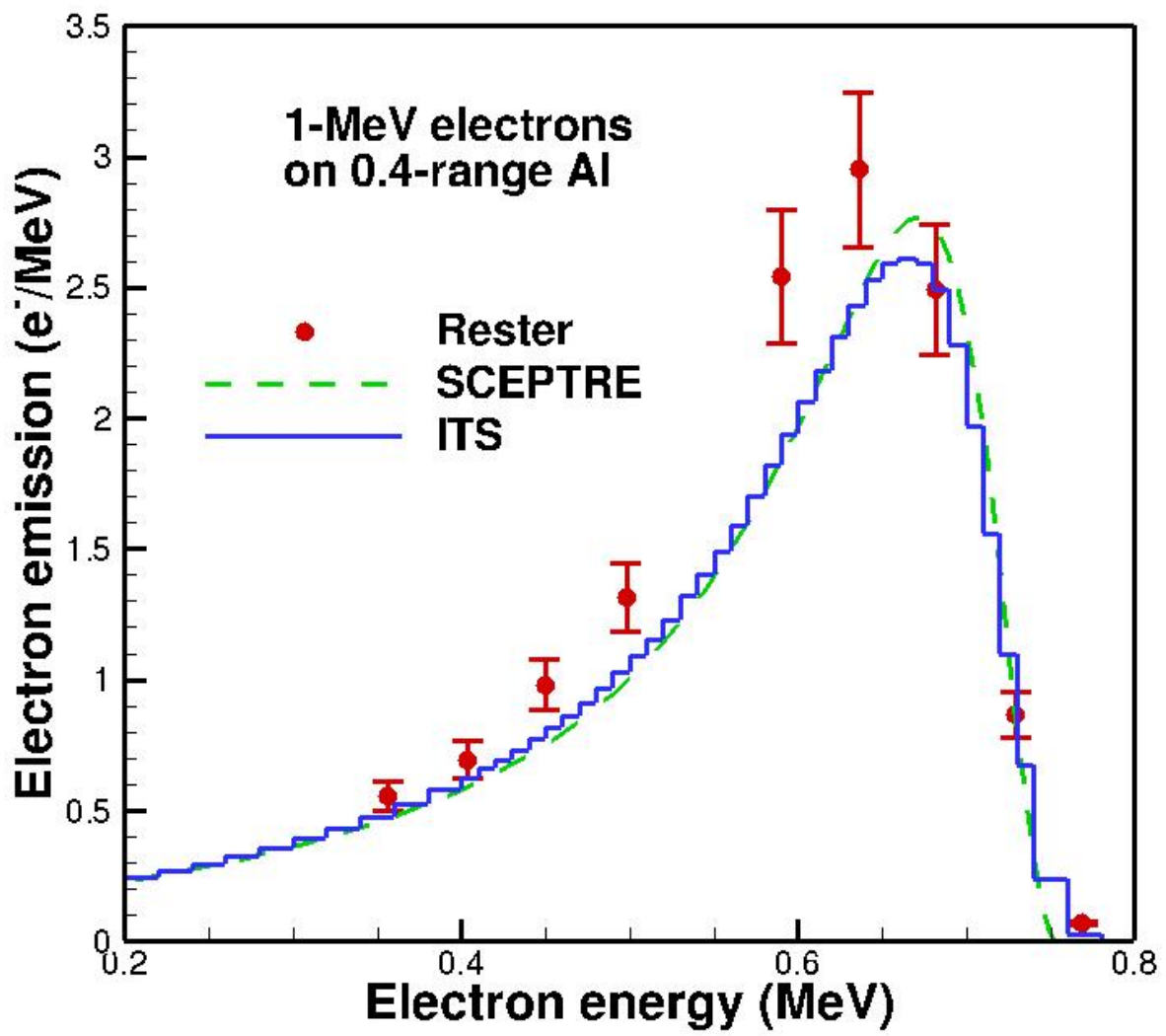


Figure 2-2 1-MeV electrons on 0.4-range Al

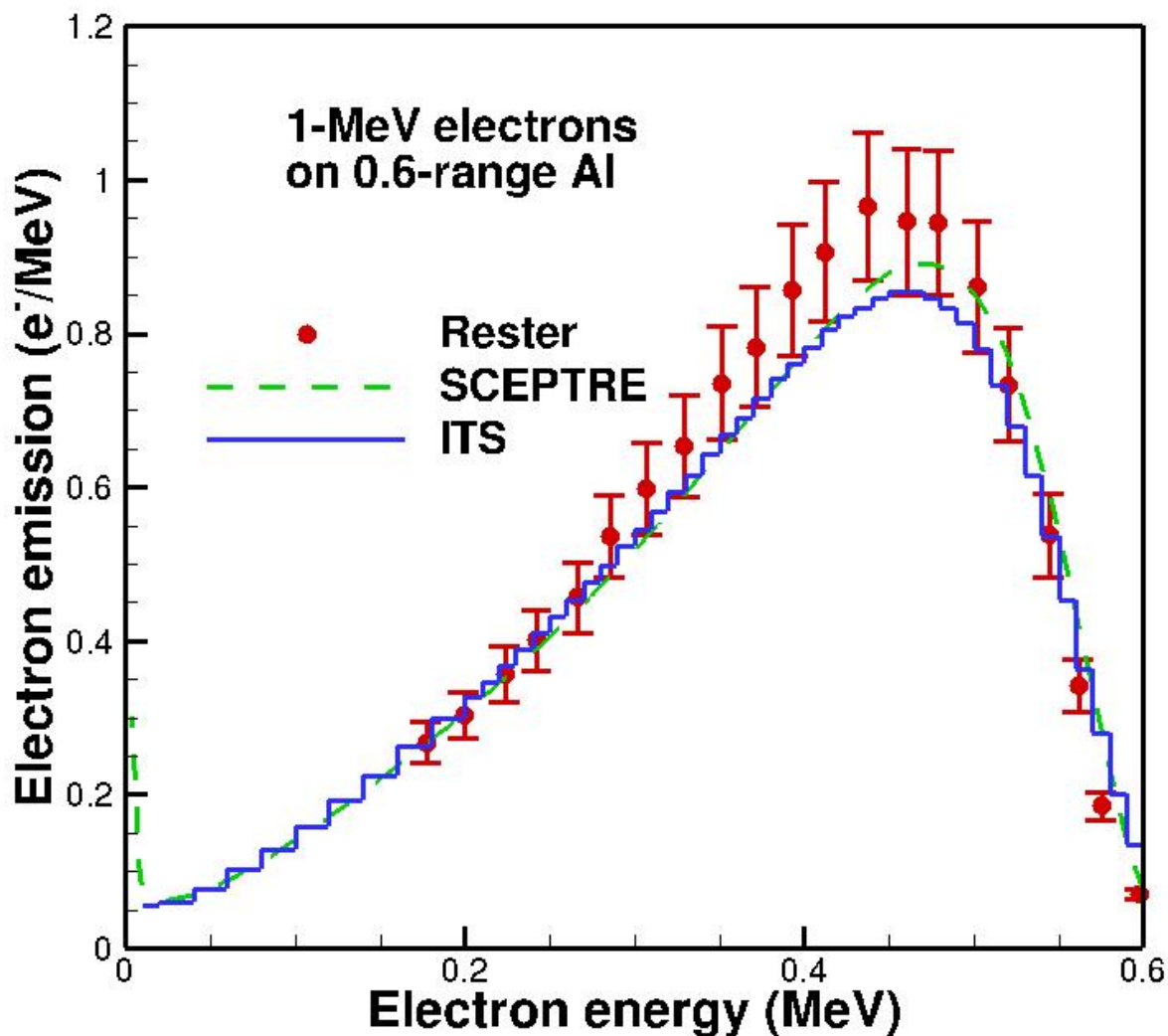


Figure 2-3 1-MeV electrons on 0.6-range Al

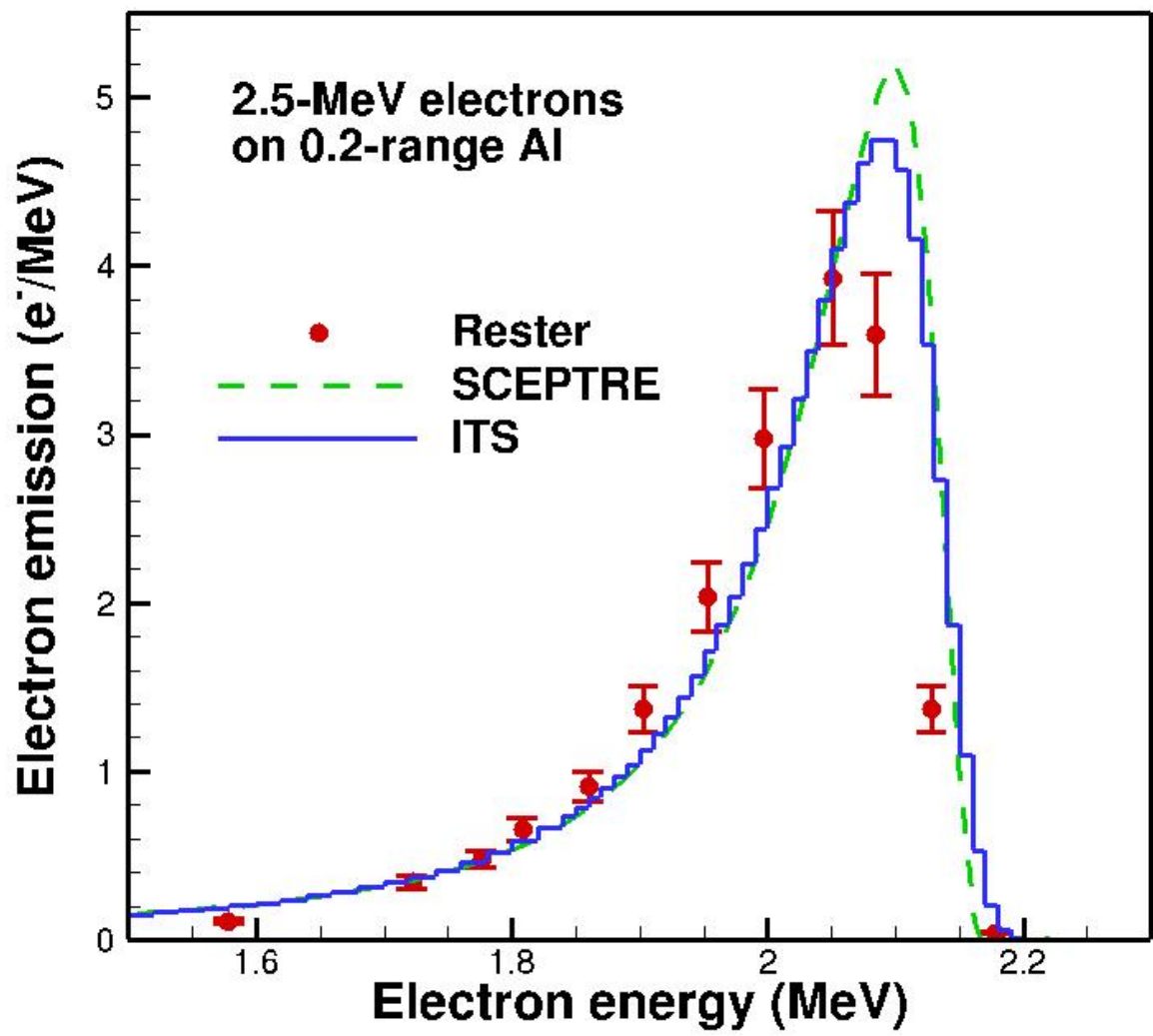


Figure 2-4 2.5-MeV electrons on 0.2-range Al

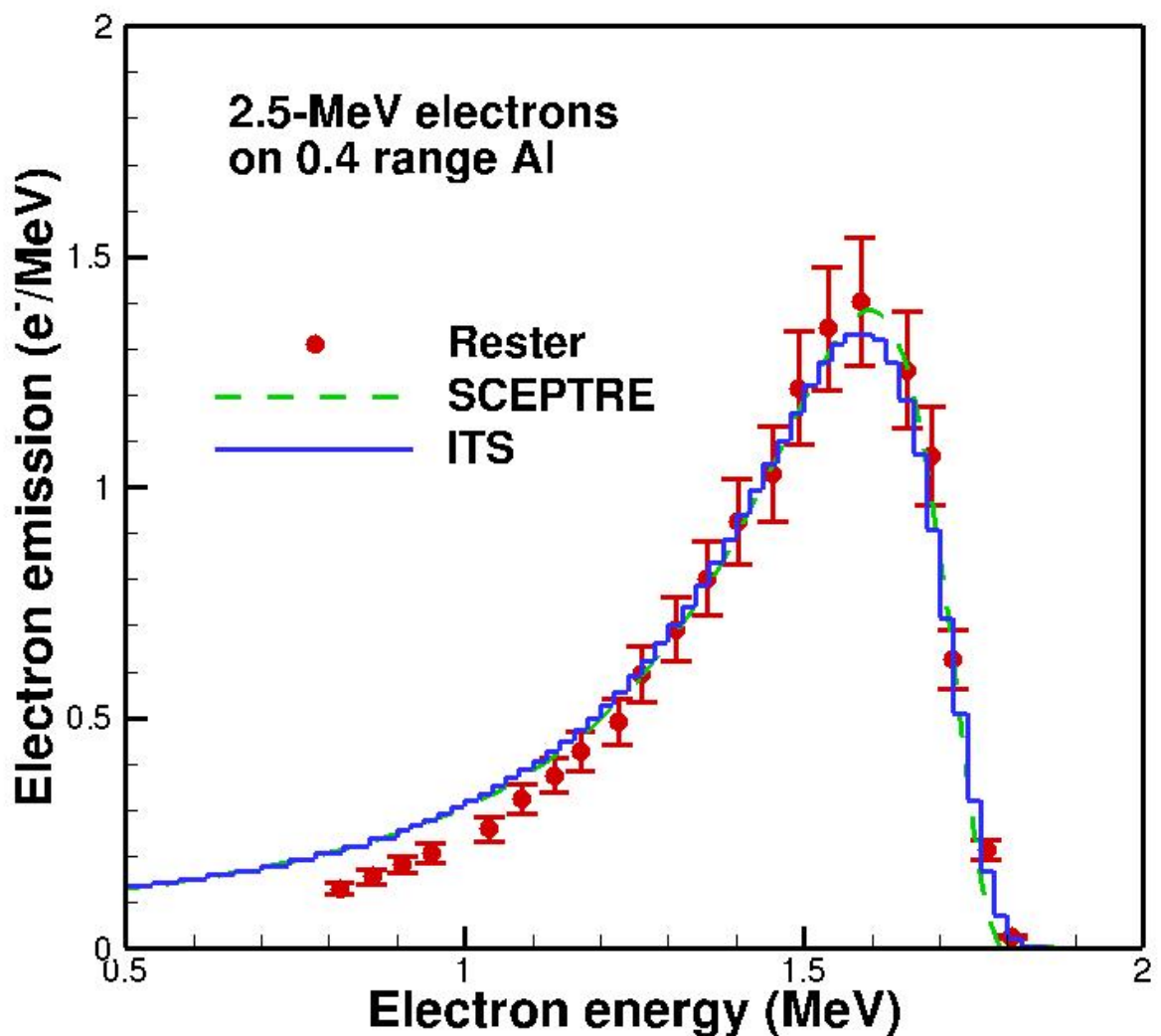


Figure 2-5 2.5-MeV electrons on 0.4-range Al

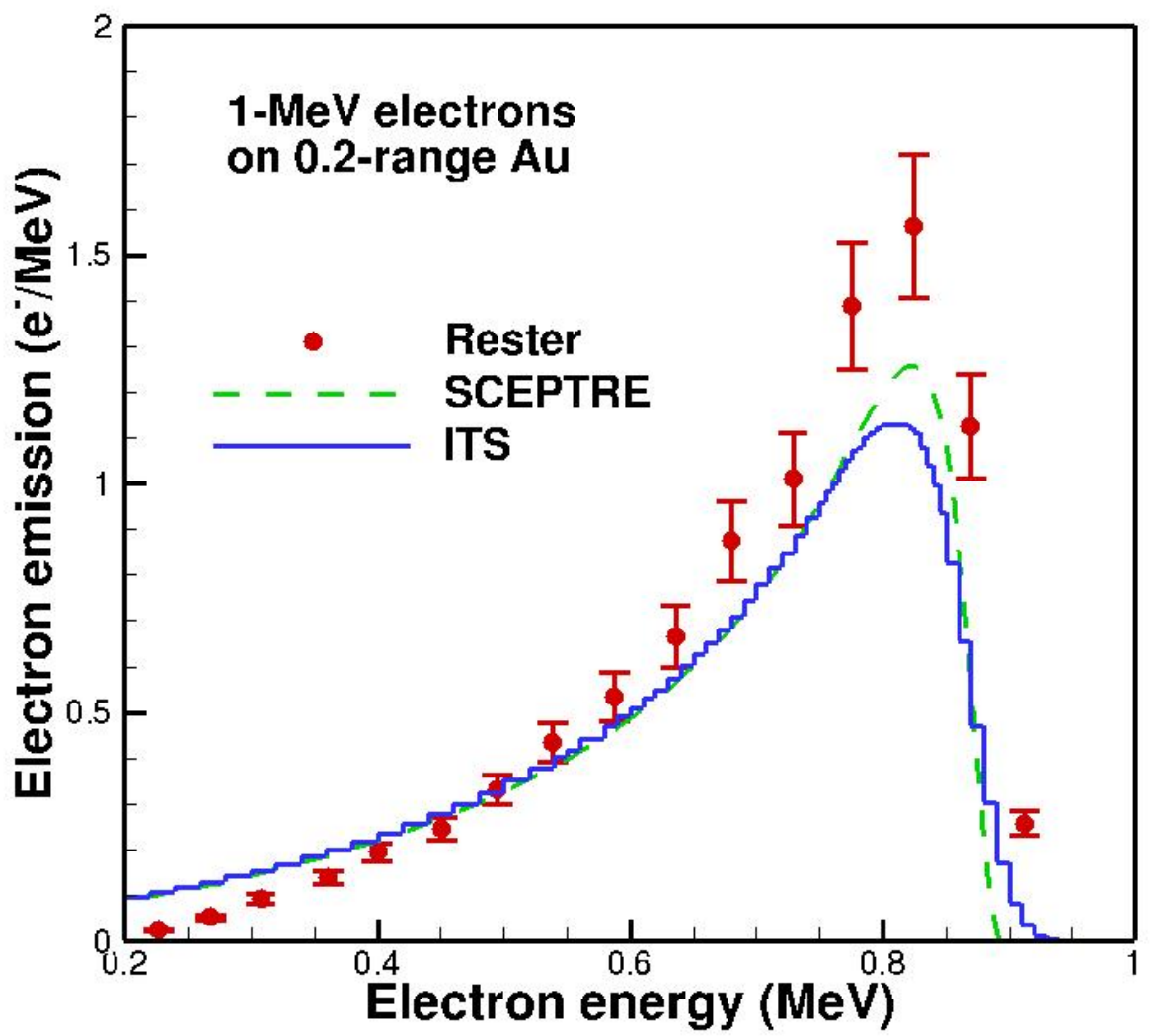


Figure 2-6 1-MeV electrons on 0.2-range Au

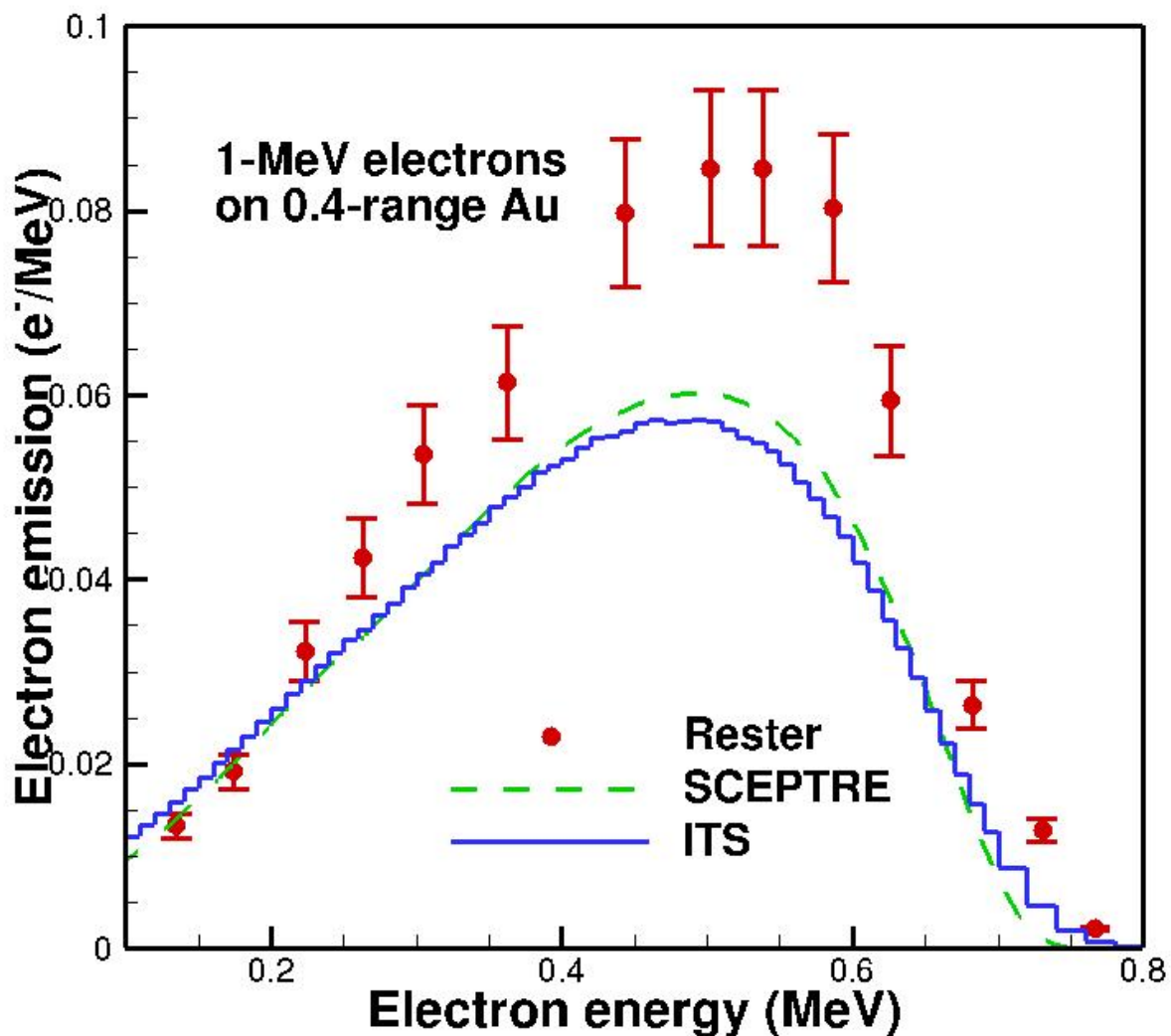


Figure 2-7 1-MeV electrons on 0.4-range Au

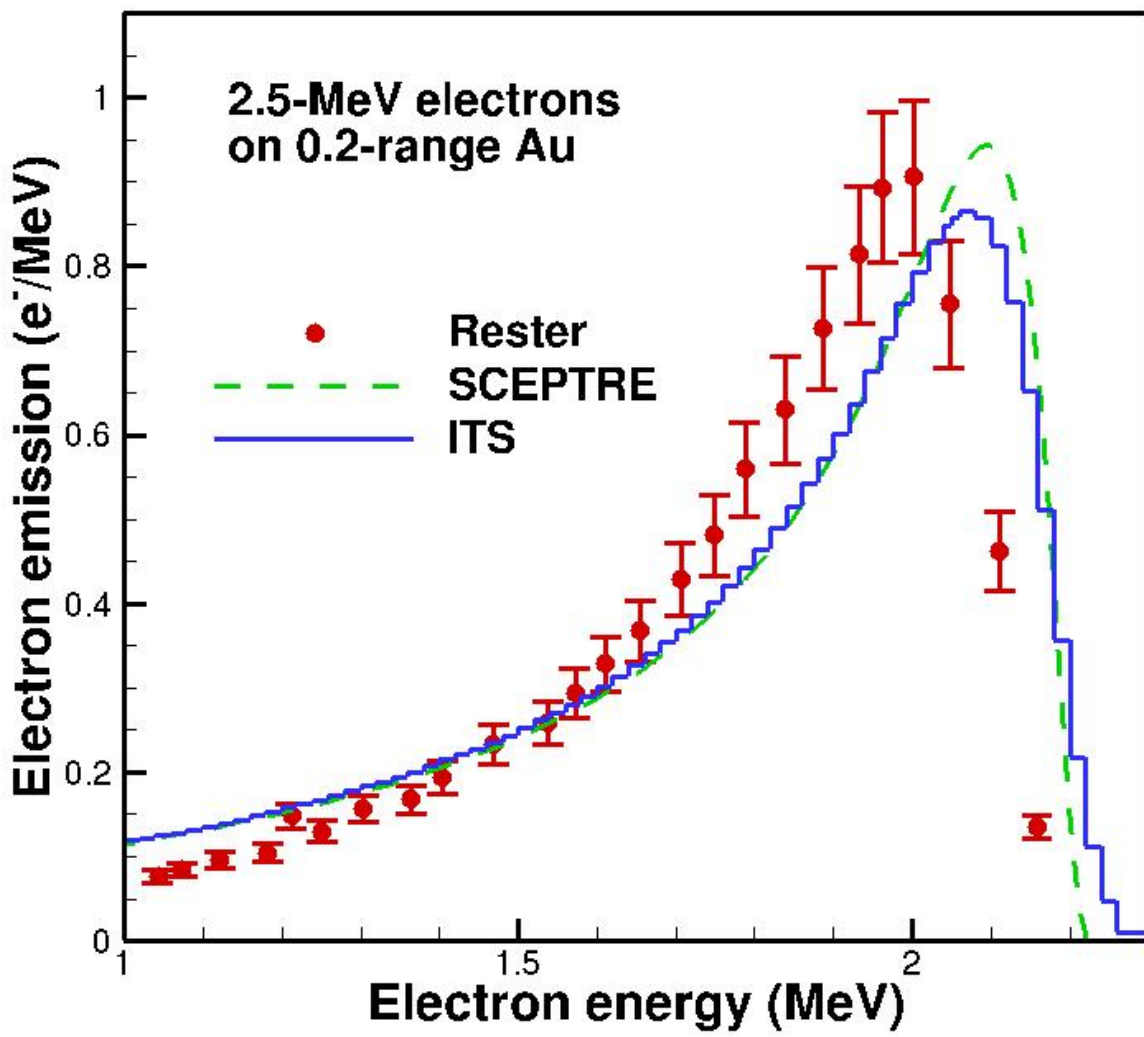


Figure 2-8 2.5-MeV electrons on 0.2-range Au

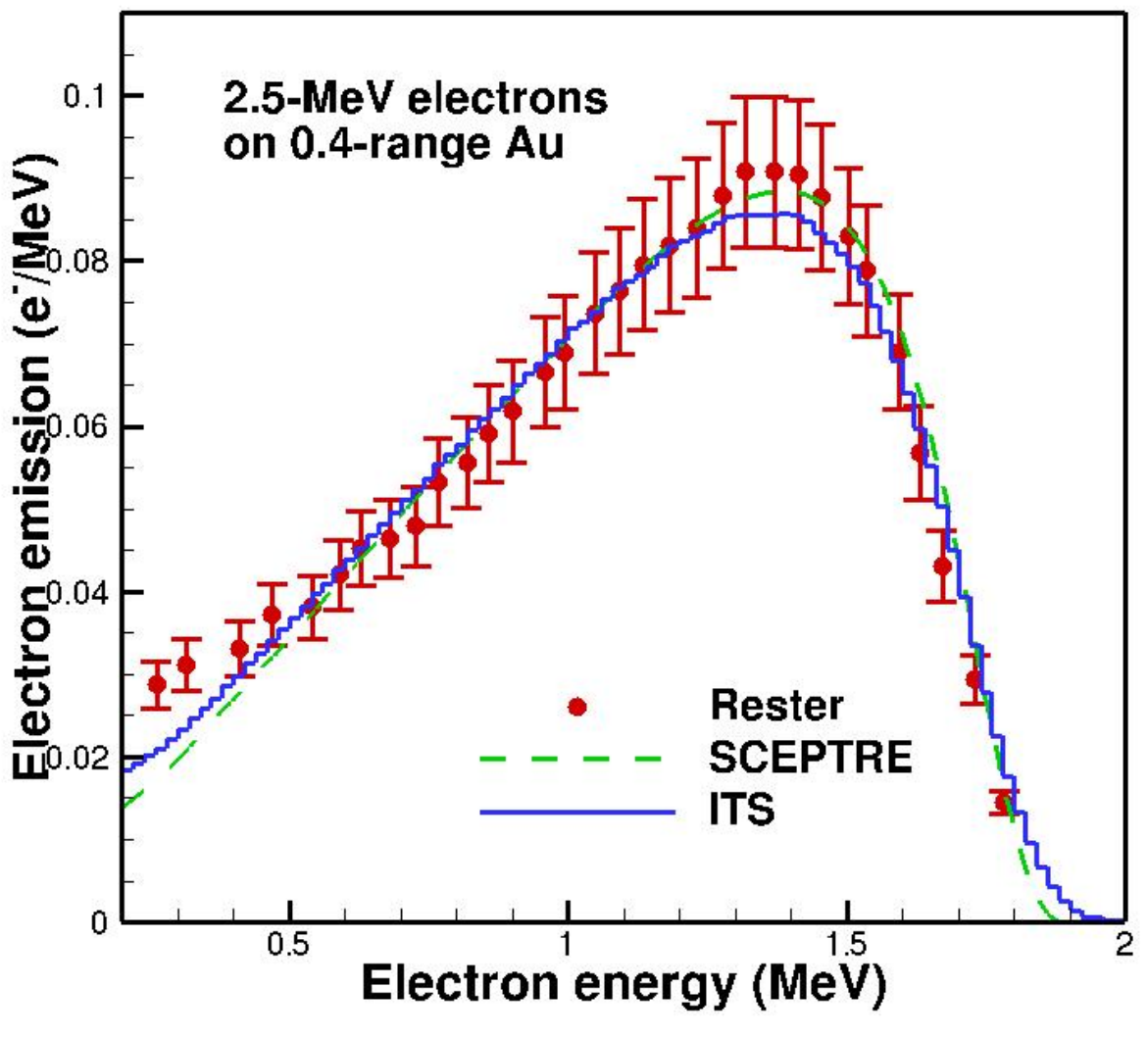


Figure 2-9 2.5-MeV electrons on 0.4-range Au

### 2.3. Rester data: sensitivity to target thickness and source energy

For several of the test configurations that had larger than average discrepancies between experiment and calculation, the effect of slightly modifying the source energy and/or target thickness was investigated. For 2.5-MeV electrons on  $\sim$ 0.2-range Al, the calculated peak intensity and location of the electron spectrum is higher than the measured peak, so the effect of increasing the target thickness by 5% was investigated. This increase in target thickness decreased the peak and average energy of the calculation, resulting in improved agreement between experiment and calculation, as shown in Fig. 2-10.

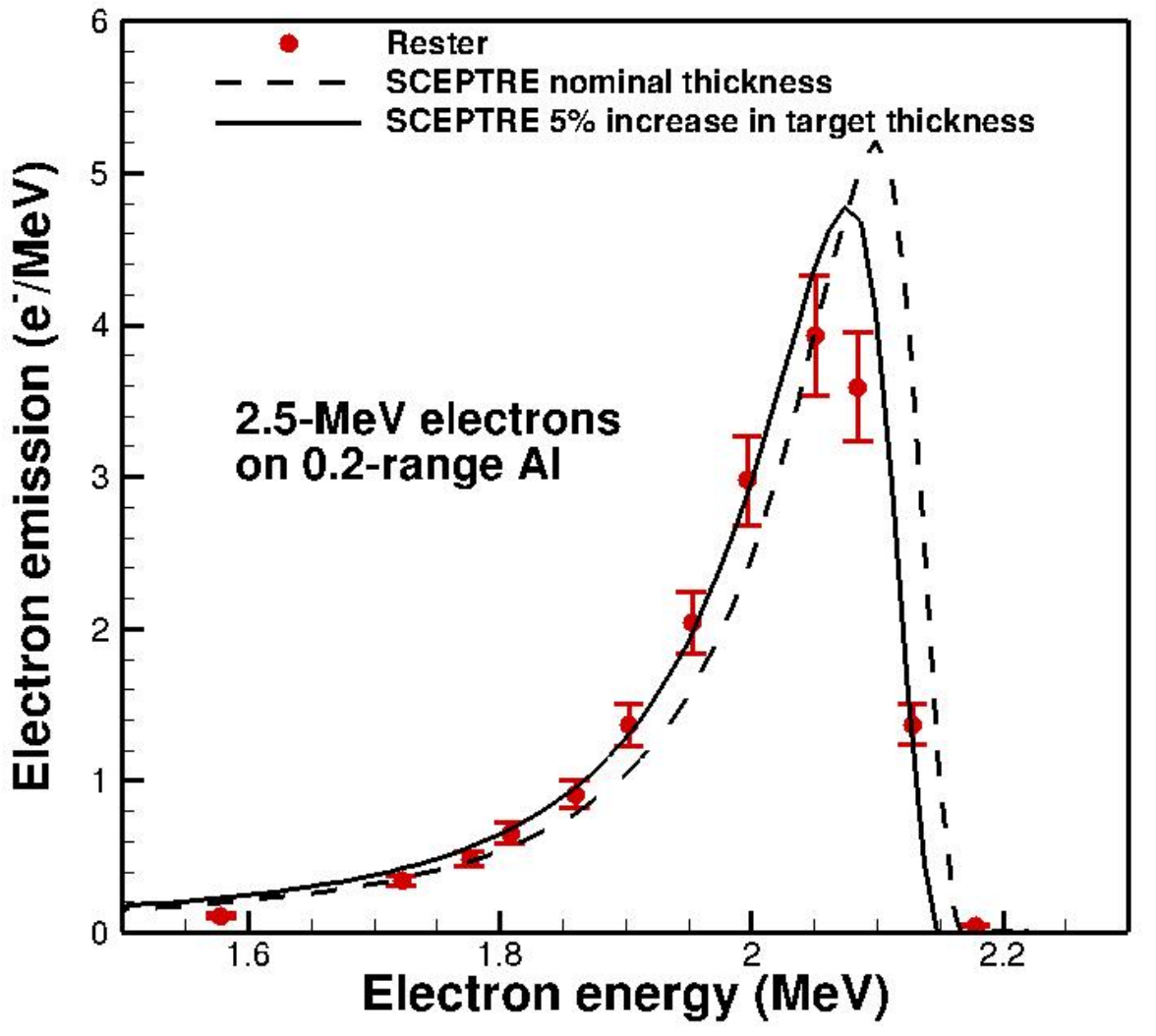


Figure 2-10 2.5-MeV electrons on 0.2-range Au with scaled target thickness

For the 1-MeV electrons on  $\sim$ 0.4-range Au, the SCEPTRE and ITS calculated results were substantially lower than the measured results, so the effect of decreasing the target thickness was investigated. Decreasing the target thickness by 4% increased the calculated peak and average energy, resulting in improved agreement between experiment and calculation, as shown in Fig. 2-11.

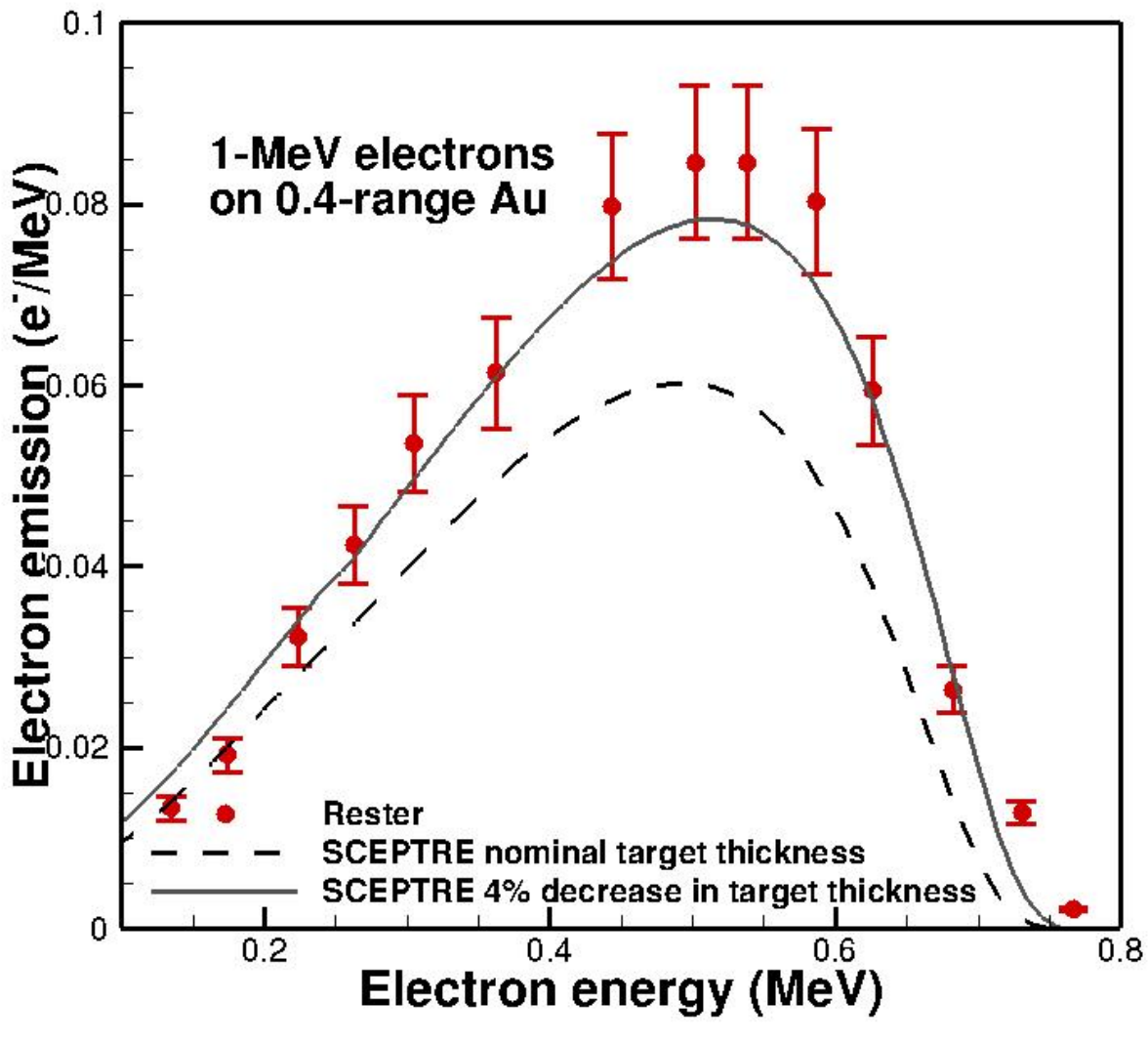


Figure 2-11 1-MeV electrons on 0.4-range Au with scaled target thickness

For 2.5-MeV electrons on  $\sim 0.2$  range Au, the energy of the calculated peak of the emission spectrum is higher than the measured result, so the effect of decreasing the source energy was investigated. Decreasing the source energy by 3% decreased the peak and average energy, resulting in improved agreement between experiment and calculation, as shown in Fig. 2-12.

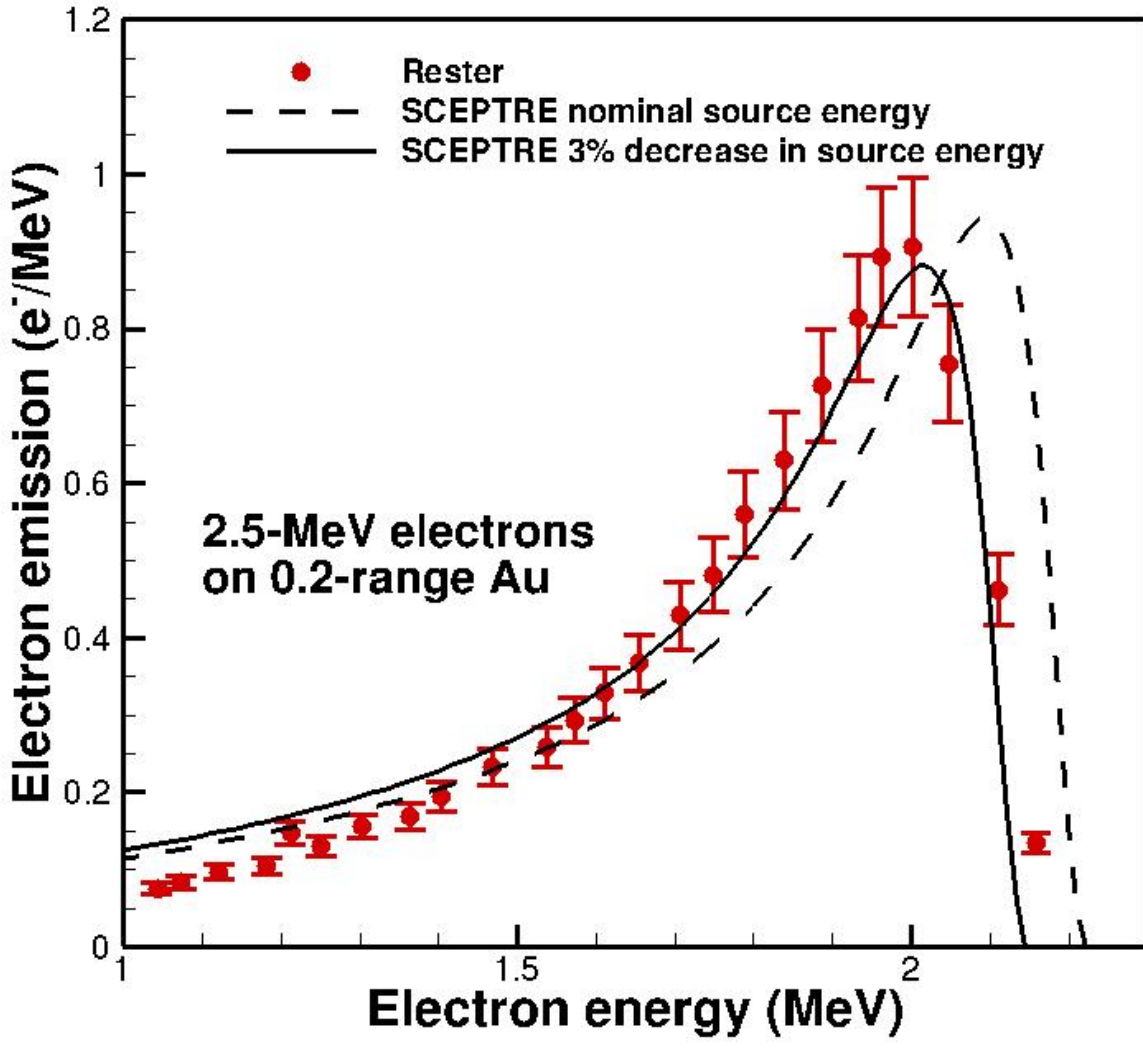


Figure 2-12 Nominal 2.5 MeV electrons on 0.2-range Au

## 2.4. Lockwood data: energy deposition profiles

A small subset of the Lockwood data [9] is compared with SCEPTRE and ITS calculational results in this section, showing good to excellent agreement. The cross sections generated by CEPXS are currently limited to electron-only Boltzmann-CSD cross sections. Performing full electron-photon radiation transport with the Boltzmann-CSD solver will require further development in the cross section generating code. For the energy-deposition calculations, neglecting photon transport results in at most about 5% overprediction of the energy deposition for high-energy electrons on high-Z targets, and relatively insignificant difference for the other test configurations. Comparison of the SCEPTRE Boltzmann-CSD results for high-energy electrons on high-Z targets will be in a future report when appropriate cross sections are available. The results presented here include coupled electron-photon ITS Monte Carlo transport calculations, and electron-only SCEPTRE Boltzmann-CSD calculations.

The SCEPTRE runs used 200 quadratic spatial elements,  $S_{16}$  angular quadrature with  $P_7$  scattering, and 200 linear energy groups, which resulted in numerical errors much less than the reported experimental uncertainty. The ITS calculations were run with sufficient histories such that the statistical uncertainties were much less than the reported experimental uncertainties. The plots include 2% error bounds on the measured data, which is approximately the average error reported. For the 0.3-MeV electrons on a tantalum target, the Lockwood report includes data obtained using two different thermal coupling models, method A and method B, and data from both methods are included in Fig. 2-18. The SCEPTRE and ITS results are in excellent agreement for all cases and also in excellent agreement with experiment for the beryllium and aluminum targets. The calculational results are about 10% higher than experimental results at the peak for the copper and tantalum targets. The reasons for these differences, which are greater than the reported uncertainties in the experimental results, are not known at the present time.

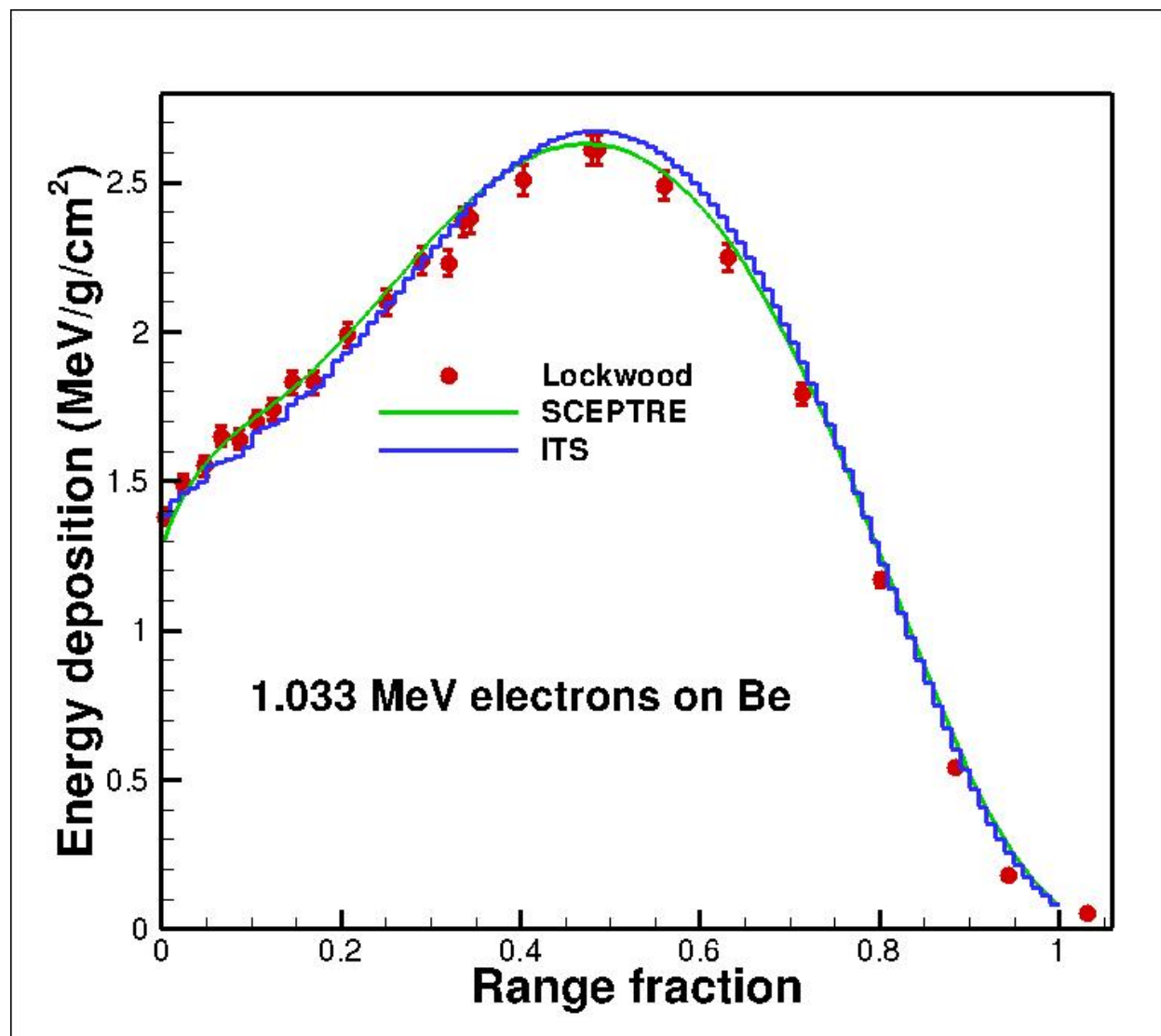


Figure 2-13 1.033-MeV electrons on range-thick beryllium

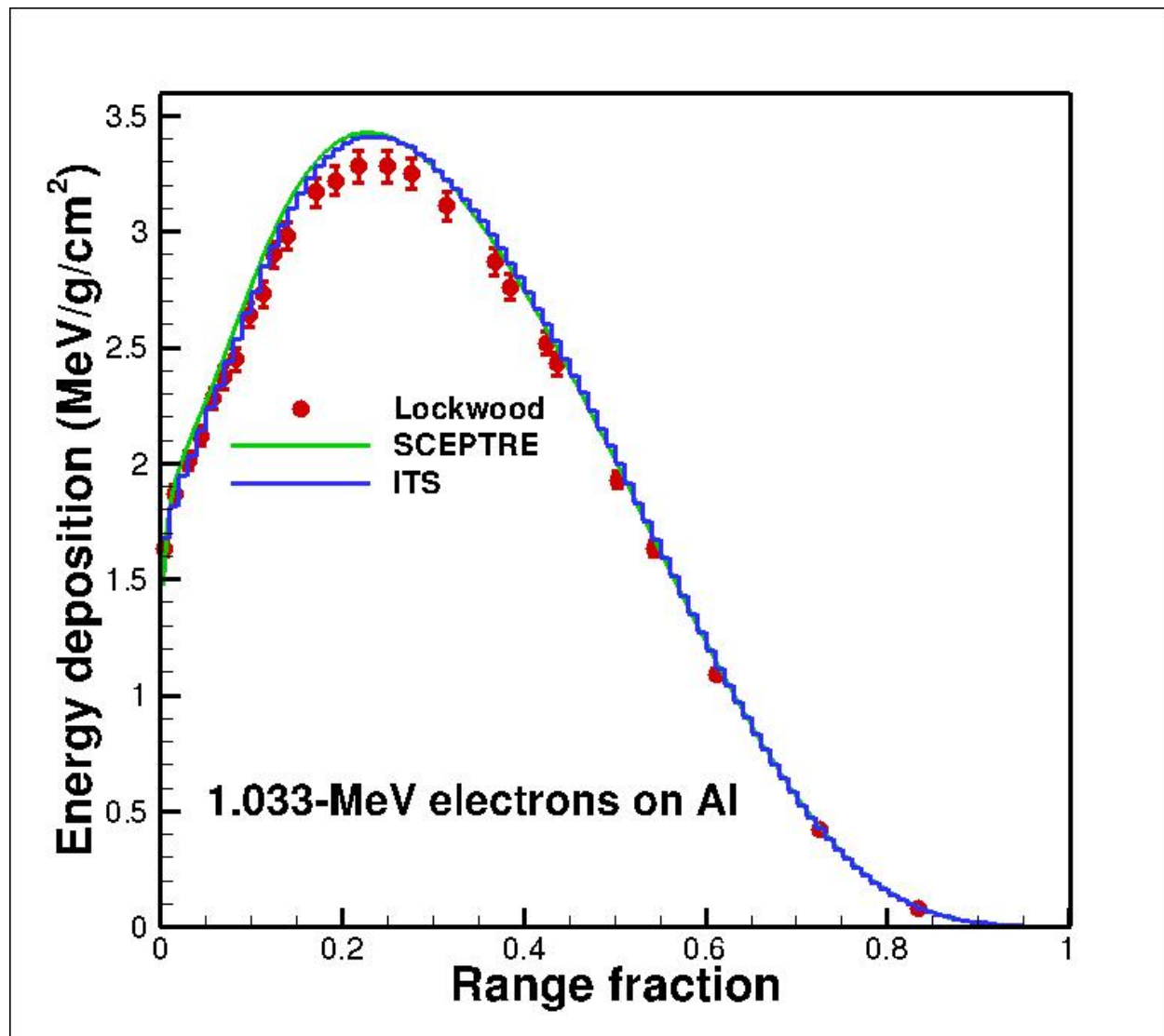


Figure 2-14 1.033-MeV electrons on range-thick aluminum

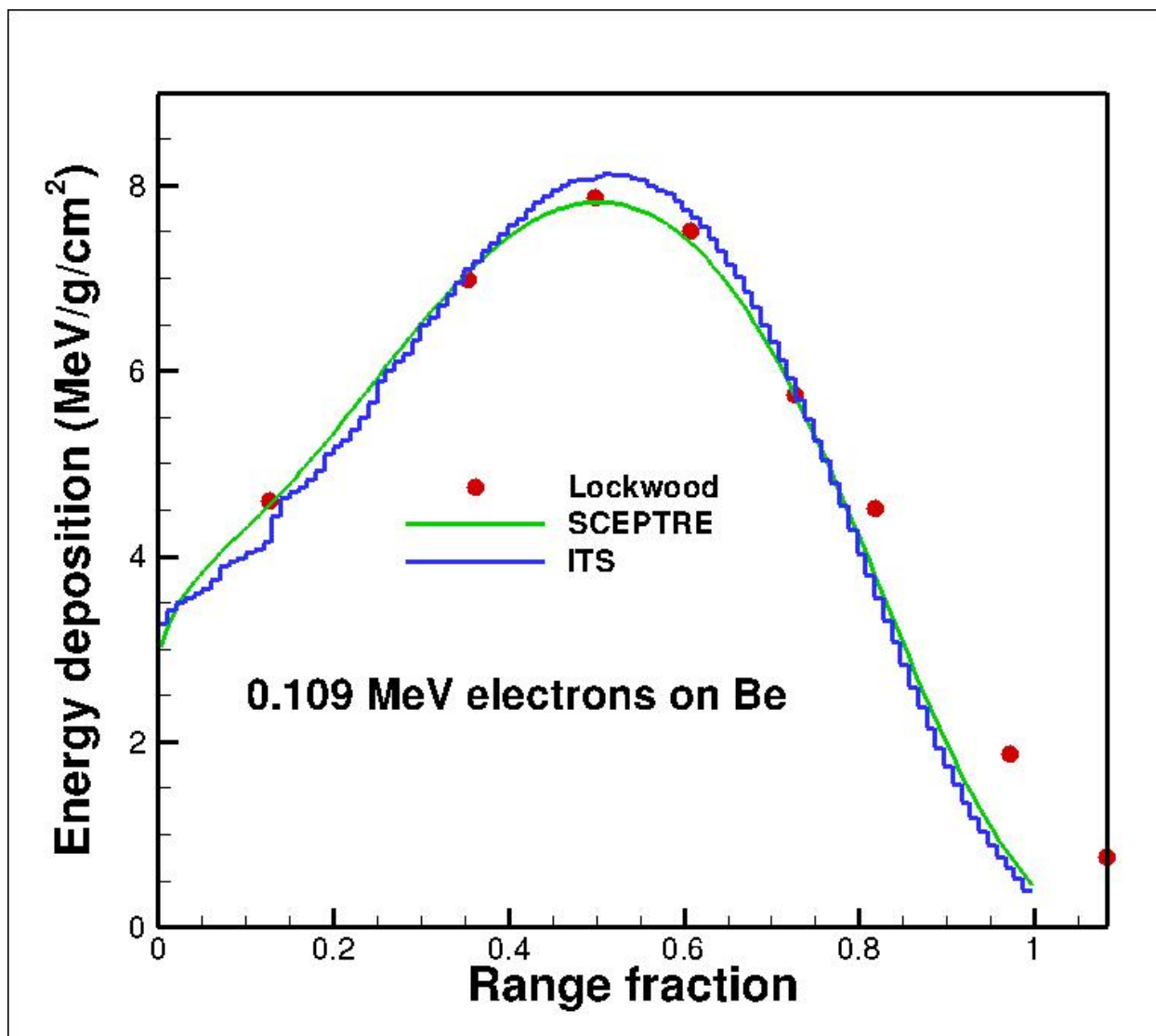


Figure 2-15 0.109-MeV electrons on range-thick beryllium

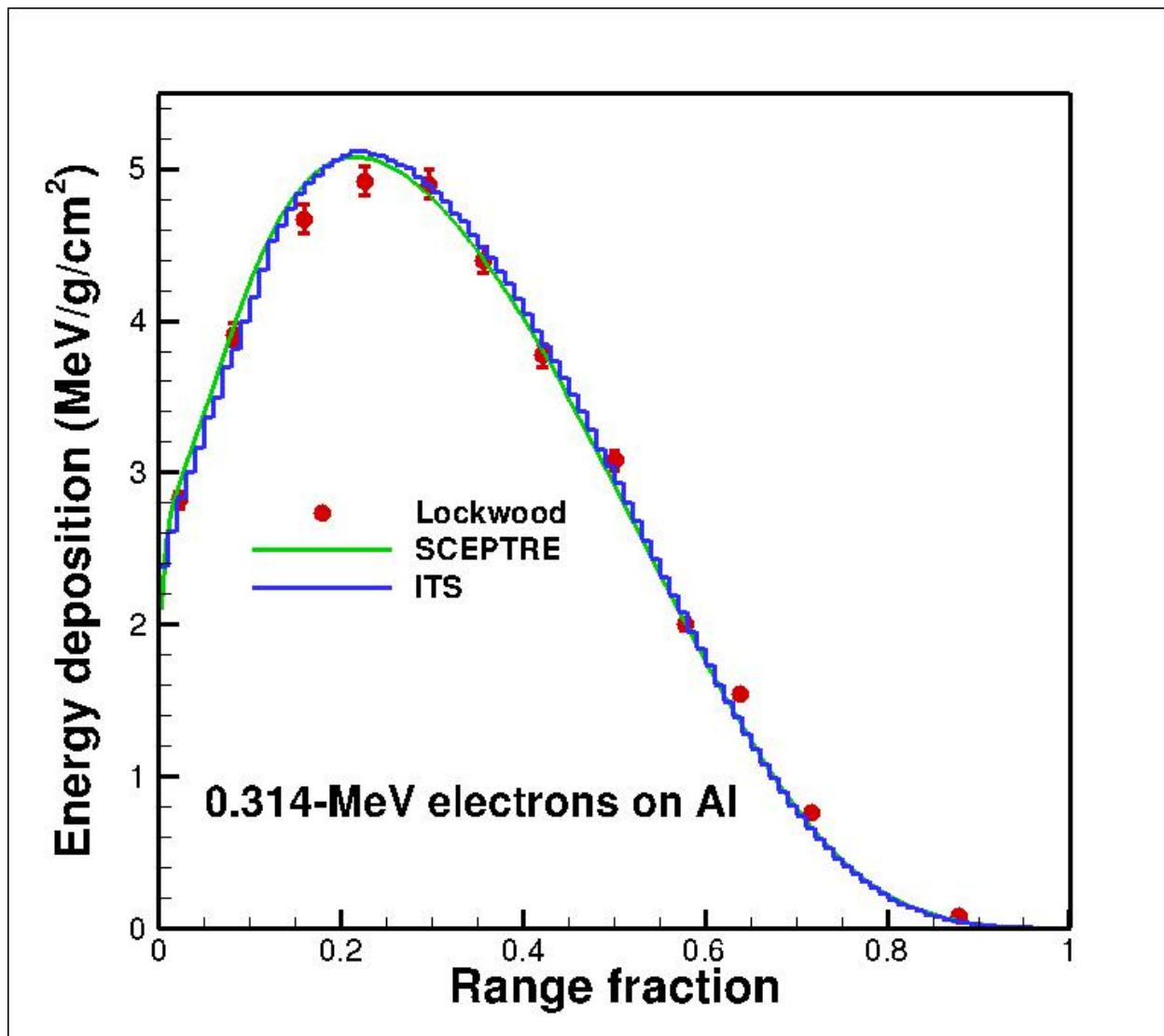


Figure 2-16 0.314-MeV electrons on range-thick aluminum

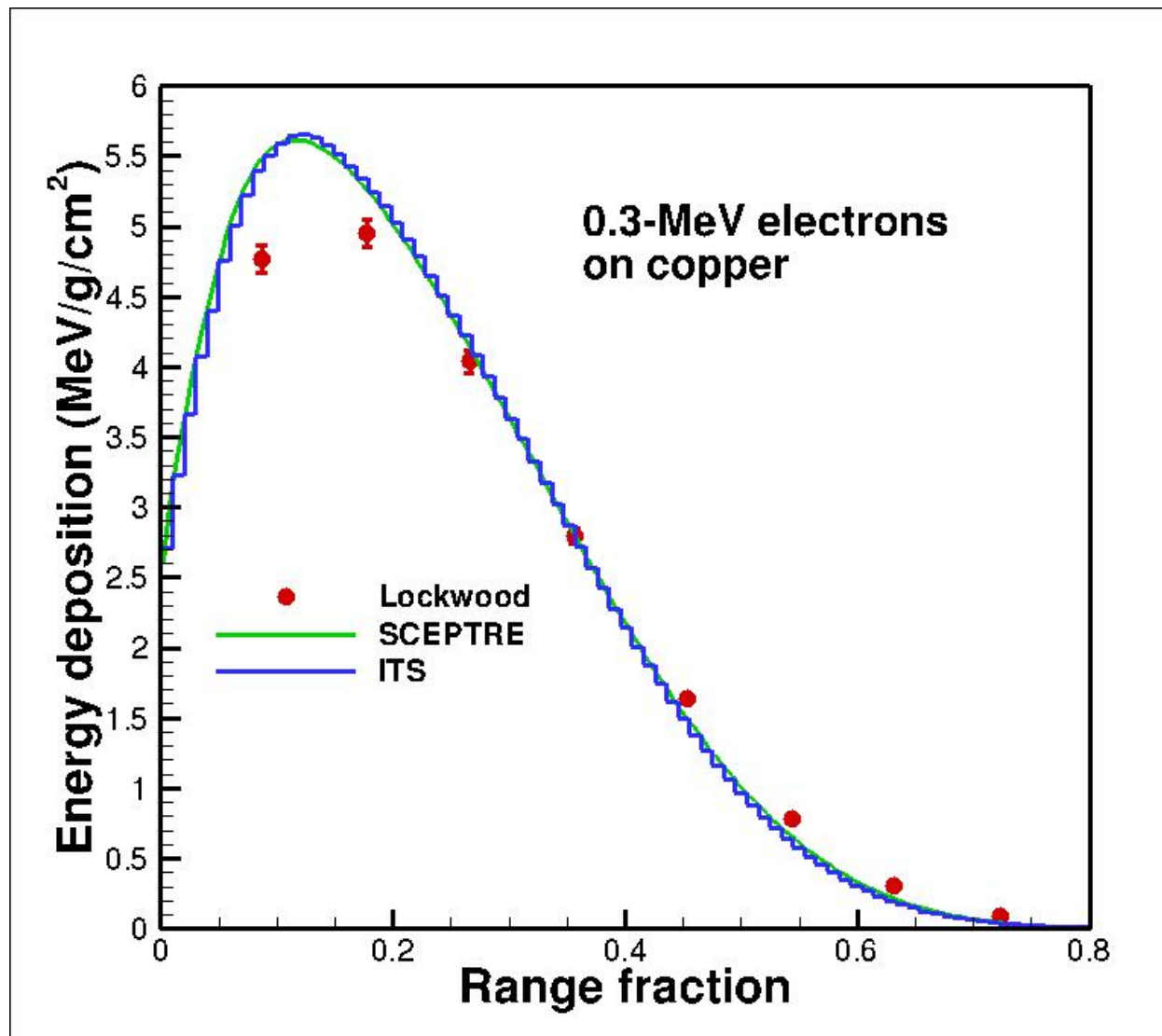


Figure 2-17 0.3-MeV electrons on range-thick copper

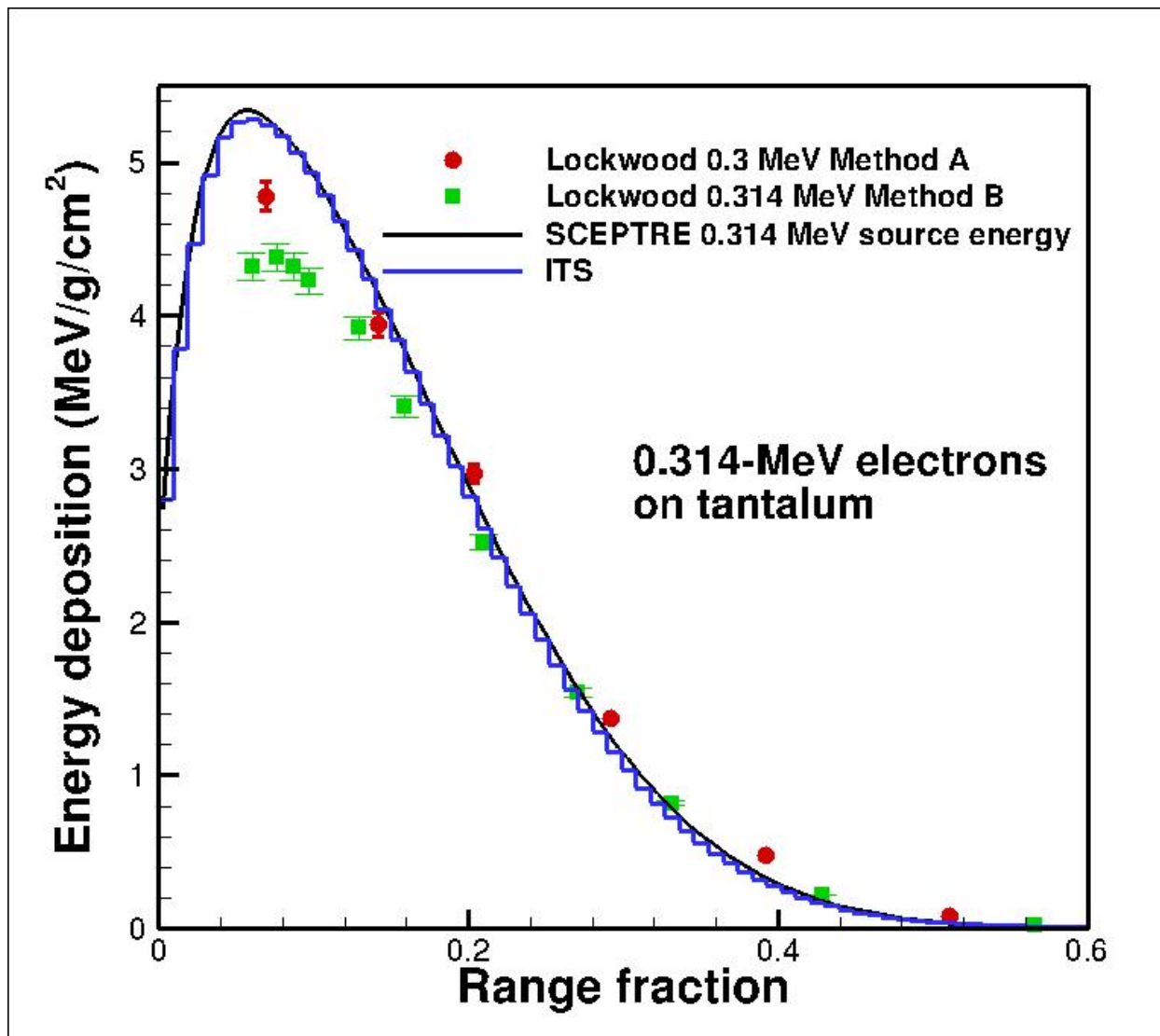


Figure 2-18 0.314-MeV electrons on range-thick tantalum

### 3. SUMMARY AND CONCLUSIONS

A new solver has been developed within SCEPTR<sup>E</sup> for solving the Boltzmann-CSD equation for charged-particle transport. The method has been validated for energy deposition and electron emission spectra by comparing calculated results with selected experimental results from two standard references. For most of the experimental configurations considered, the SCEPTR<sup>E</sup> Boltzmann-CSD results compare well with experiment and ITS Monte Carlo results. The SCEPTR<sup>E</sup> Boltzmann-CSD solver relies on electron cross sections generated by the legacy CEPXS code, which currently is limited to electron-only Boltzmann-CSD cross sections. Performing full electron-photon radiation transport with the Boltzmann-CSD solver will require further development in the cross section generating code. For the energy-deposition calculations, neglecting photon transport results in at most about 5% overprediction of the energy deposition for high-energy electrons on high-Z targets, and relatively insignificant difference for the other test configurations. Validation of the Boltzmann-CSD solver for test configurations requiring coupled electron-photon transport will be performed when appropriate cross sections are available.

## REFERENCES

- [1] D. Bruss, et al., "SCEPTRE 2.2 Quick Start Guide," Sandia National Laboratories report, SAND2021-3073 (2021).
- [2] J. Morel, "Fokker-Planck Calculations Using Standard Discrete Ordinates Transport Codes", *Nucl. Sci. Eng.* **79**, 340-356 (1981).
- [3] L. Lorence, et al., "Physics guide to CEPXS: A multigroup coupled electron-photon cross-section generating code," Sandia National Laboratories report, SAND89-1685 (1989).
- [4] J. Duderstadt and W. Martin, *Transport Theory*, Wiley-Interscience, New York (1979).
- [5] J. Tervo, et al., "On existence of solutions for Boltzmann Continuous Slowing Down transport equation," *J. Math. Anal. and App.*, 460, 271 (2018).
- [6] J. Powell, et al, "Finite Element Solution of the Self-Adjoint Angular Flux Equation for Coupled Electron-Photon Transport," *Nucl. Sci. Eng.* **142**, 270-291 (2002).
- [7] B. Franke, et al., "ITS Version 6.7: The Integrated TIGER Series of Coupled Electron/Photon Monte Carlo Transport Codes," Sandia National Laboratories report, SAND2008-3331 (2008).
- [8] D. Rester and J. Derrickson, "Electron Transmission Measurements for Al, Sn, and Au Targets at Electron Bombarding Energies of 1.0 and 2.5 MeV," *J. Appl. Phys.* **42**, 714 (1971).
- [9] G. Lockwood, et al., "Calorimetric Measurement of Electron Energy Deposition in Extended Media—Theory Vs. Experiment," Sandia National Laboratories report, SAND79-0414 (1980).

## DISTRIBUTION

### Email—Internal

Name	Org.	Sandia Email Address
Joseph Castro	01341	<a href="mailto:jpcastr@sandia.gov">jpcastr@sandia.gov</a>
Kerry Bossler	01341	<a href="mailto:kbossle@sandia.gov">kbossle@sandia.gov</a>
Donald Bruss	01341	<a href="mailto:dbruss@sandia.gov">dbruss@sandia.gov</a>
Clifton Drumm	01341	<a href="mailto:crdrumm@sandia.gov">crdrumm@sandia.gov</a>
Jarrod Edwards	01341	<a href="mailto:jdedwa@sandia.gov">jdedwa@sandia.gov</a>
Wesley Fan	01341	<a href="mailto:wcfan@sandia.gov">wcfan@sandia.gov</a>
Brian Franke	01341	<a href="mailto:bcfrank@sandia.gov">bcfrank@sandia.gov</a>
Ronald Kensek	01341	<a href="mailto:rpkense@sandia.gov">rpkense@sandia.gov</a>
Luke Kersting	01341	<a href="mailto:likerst@sandia.gov">likerst@sandia.gov</a>
Aaron Olson	01341	<a href="mailto:aolson@sandia.gov">aolson@sandia.gov</a>
Technical Library	01977	<a href="mailto:sanddocs@sandia.gov">sanddocs@sandia.gov</a>

This page left blank

This page left blank



**Sandia  
National  
Laboratories**

Sandia National Laboratories is a multimission laboratory managed and operated by National Technology & Engineering Solutions of Sandia LLC, a wholly owned subsidiary of Honeywell International Inc. for the U.S. Department of Energy's National Nuclear Security Administration under contract DE-NA0003525.